Bioleaching of sulfide containing material from the Wiśniówka Quarry: stability and adhesion of secondary products

Agnieszka Pawlowska [1], Zygmunt Sadowski [1], Katarzyna Winiarska [2]

[1] Department of Process Engineering and Technology of Polymer and Carbon Materials, Wrocław University of Science and Technology, Wybrzeże Wyspiańskiego 27, 50-370 Wrocław, Poland

[2] Department of Analytical Chemistry and Chemical Metallurgy, Wrocław University of Science and Technology, Wybrzeże Wyspiańskiego 27, 50-370 Wrocław, Poland

Corresponding author: agnieszka.pawlowska@pwr.edu.pl

Abstract: Secondary products (minerals) formed during bioleaching play an essential role in this process. Their adhesion to the surface of leached grains can inhibit bioleaching. For this reason, it is crucial to know the physicochemical conditions of adhesion. Selected material from the Wiśniówka Quarry (Kielce, Poland) with increased content of sulfides was subjected to microbial leaching. A precipitate collected from a bacterial culture was used as a secondary product (mainly jarosite). Adhesion and bio-extraction tests were carried out in a column reactor with a mineral bed (particle size 0.8 - 1.2 mm). The cationic surfactant (CTAB), anionic surfactant (SDS), and rhamnolipids (RL) were used to modify the surface of minerals and secondary products. Changes in the surface properties were determined with zeta potential measurements. The cationic surfactant above the 0.5 mM caused stability of jarosite suspension. Also, bioleaching efficiency was the highest for mineral surfaces modified by CTAB. The quantitative interpretation of the adhesion of the secondary product to bioleach mineral material was carried out.

Keywords: bioleaching, As-bearing waste, secondary product, jarosite, adhesion, stability, zeta potential

1. Introduction

Acid mine drainage (AMD) is sulfuric-rich wastewater that arises during bioleaching. The ionic composition of the leaching effluent depends on the mineral being leached (Akcil and Koldas, 2006; Johnson and Hallberg, 2005). Generally, such waste contains an elevated concentration of metal and metalloid ions. For example, a typical bioleach solution from gold ore pretreatment contains more than 10 g/L of As and 20 g/L of Fe (Lee and Chon, 2006). When the high ion concentration exceeds the solubility product constants, secondary minerals precipitate (Battaglia-Brunet et al., 2012). Their role in the bioleaching process is still not fully understood.

Various secondary products have been identified in the AMD solution, including schwertmannite, jarosite, and goethite (Hammarstrom et al., 2005). Its type depends on the mineral composition of the solid being bioleached. Since mine leachates contain a high concentration of ferric and sulfate ions, schwertmannite, a weakly crystalline Fe(III) oxyhydroxysulfate mineral $Fe_8O_8(OH)_6SO_4$), can precipitate (Khamphila et al., 2017). It is a metastable compound, formed at pH 2.8-4.5, converting to goethite at higher pH (Houngaloune et al., 2014; Pawlowska and Sadowski, 2020). It may also be a precursor to jarosite formation (Sandy Jones et al., 2014). The solubility of Fe^{3+} ions in the leachate is pH-dependent. At high SO_4^{2-} ion concentration and pH below 2.8, jarosite precipitates. The chemical formula of this secondary mineral is $MFe_3(SO_4)_2(OH)_6$, where M can be Na^+, K^+, NH_4^+, and H_3O^+, which are dominant monovalent cations (Kaksonen et al., 2014). The particles of the secondary product form a compact layer on the leached mineral and inhibit biooxidation. It was shown that the biooxidation of Fe(II) and the jarosite formation are directly related. The operating conditions for the ferrous iron oxidation by *Acidithiobacillus ferrooxidans*, under which a minimal amount of jarosite was formed, were a temperature of 35 °C and pH 1.6-1.7 (Daoud and Kalamanov, 2006).

Other secondary iron oxyhydroxide minerals, such as goethite (α-FeOOH) and akageneite (β-FeOOH) precipitate at different pH (Egal et al., 2009; Jönsson et al., 2006). The first is formed at circumneutral pH, the second at room temperature, and a pH between 1.2 and 1.4 (Deliyanni et al., 2001; Jönsson et al., 2005).

During bioleaching of arsenic-bearing minerals, iron(III) ions react with the arsenic ions present in the solution, leading to scorodite formation (Drahota and Filippi, 2009). Precipitation of this secondary product is a standard method of extracting arsenic ions from dilute industrial solutions (Caetano et al., 2009). Effective removal of arsenic from the AMD solution requires the following condition: oxidation of arsenic(III) ions and appropriate As/Fe ratio. Chemoautotrophic bacteria ensure that arsenic(III) is oxidized to arsenic(V), and the presence or extra addition of iron(III) salt causes the As/Fe ratio to reach the value 1 (Paikaray, 2015).

The scientific literature uses another term, "acid rock drainage" (ARD), which refers to the effects of rock and mineral biooxidation. Pyrite is the most abundant sulfide mineral and is a component of sulfide ores. One mol of pyrite exposed to oxidizing conditions produces 4 mol of protons (Dold, 2017). The liberated Fe^{2+} ions are oxidized by *Acidithiobacillus* or *Leptospirillum*, and analogously to AMD, precipitation of secondary products occurs.

This work aims at showing the physicochemical properties of jarosite and ammoniojarosite and their stability and adhesion during the bioleaching process and explaining the role of cationic and anionic surfactants and biosurfactants.

2.   Materials and methods

2.1.   Mineral sample

The mineral material used in this research was obtained from the Wiśniówka Quarry (south-central Poland) and sorted by hand to enrich it with sulfide minerals. The collected rock was mechanically crushed and separated into particle size fractions. The 0.8 - 1.2 mm fraction was used for bioleaching and adhesion studies. The elemental analysis identified by XRF (ARL QUANT'X EDXRF analyzer, Thermo Fisher Scientific) and oxide content of the Wiśniówka Quarry are shown in Table 1 and Table 2, respectively. The phase composition was investigated by powder X-ray diffraction (Empyrean, PANalytical) and based on the diffraction pattern PDF4+ 2019. The main compounds of Wiśniówka mineral material are SiO_2 (65.2%) and Fe_2O_3 (21.59%), with high content of sulfur (13.66%) and iron (7.13%), which make it suitable for microbial extraction using *A. ferrooxidans*. XRD diffractogram (Fig. 1) shows peaks originating from pyrite (FeS_2), quartz (SiO_2), muscovite ($K(Al_4Si_2O_9(OH)_3)$) and dickite ($Al_2Si_2O_5(OH)_4$) developed by weathering of the last.

Table 1. XRF analysis of mineral material from Wiśniówka Quarry

Element	Si	S	Fe	P	Al	K	As	Ti	Ca
Content [m/m%]	40.7	13.66	7.13	2.26	2.1	1.36	0.998	0.337	0.19

Table 2. Oxide content of the mineral material from Wiśniówka Quarry

Compound	SiO_2	Fe_2O_3	Al_2O_3	CaO
Content [%]	65.2	21.59	8.86	2.1

2.2. Secondary product synthesis and size distribution

Jarosite $KFe_3(SO_4)_2(OH)_6$ was obtained as a precipitate collected from the cultivation of *A. ferrooxidans*. 9K medium with the following composition (for 1 litre of deionized water): $FeSO_4 \cdot 7H_2O$ 44.8 g, $(NH_4)_2SO_4$ 3.0 g, K_2HPO_4 0.5 g, $MgSO_4 \cdot 7H_2O$ 0.5 g, KCl 0.1 g, $Ca(NO_3)_2$ 0.01 g was used for bacterial growth. The pH of the medium was maintained with 5 M H_2SO_4. The secondary product was mixed, dried, and examined by the X-ray diffraction method to identify the solid product (Fig. 2). Jarosite and ammoniojarosite were detected on the diffractogram. The second one results from ammonium salts present in the medium used for bacteria cultivation.

The powder particle size analysis of jarosite was carried out with the application of an LS 13 320 Beckman Coulter (USA) equipped with the Universal Liquid Module (ULM). The particle size distribution was determined with laser diffraction (pump speed 100%; optical model: Fraunhofer.rf780d; residual 0.78%; obscuration 12%). The sample was suspended in a 10^{-3} M NaCl solution. The mean and median particle size was 2.815 µm and 1.650 µm, respectively (Fig. 3).
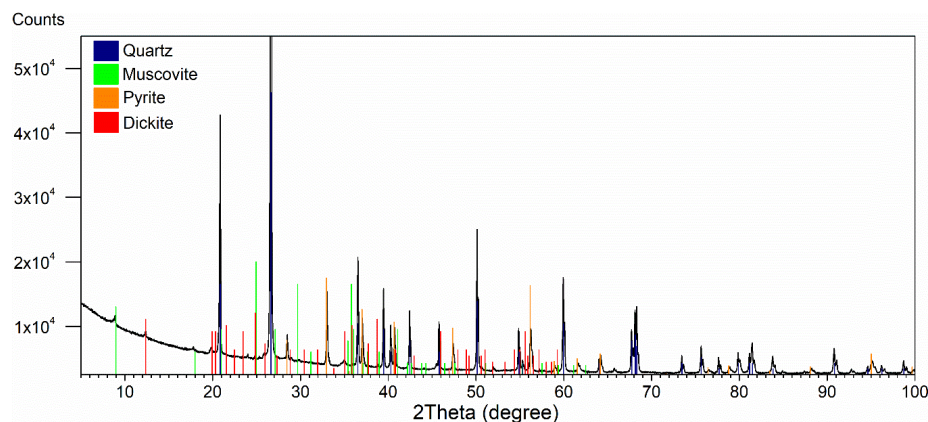

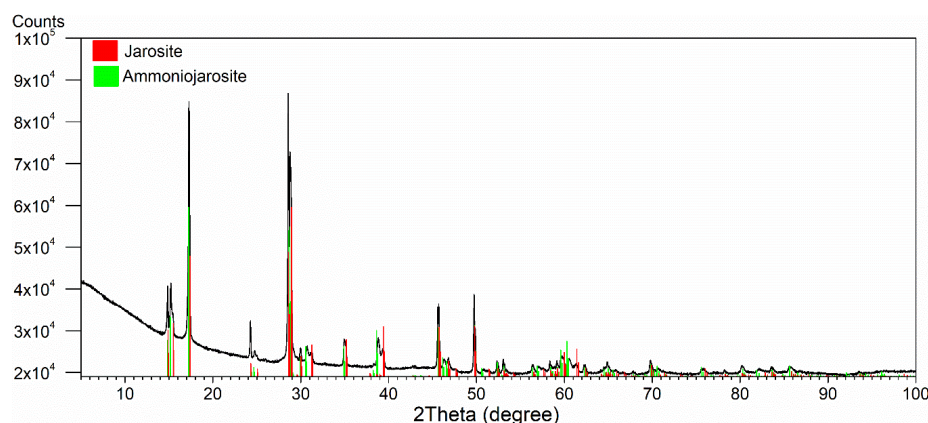Fig. 1. XRD analysis of Wiśniówka Quarry material

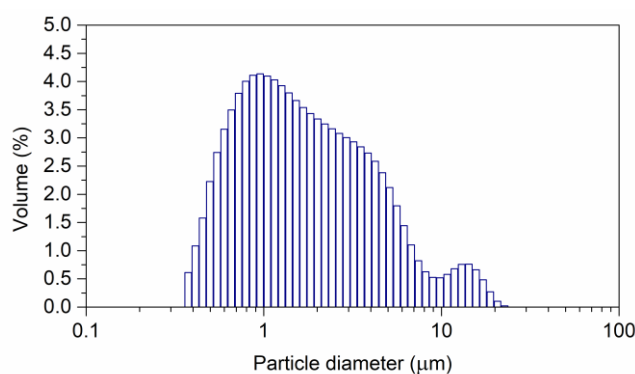Fig. 2. XRD analysis of the secondary product

Fig. 3. Size distribution of the secondary product (jarosite)

2.3. Surfactants and biosurfactants

The rhamnolipid (RL) used in the experiments was purchased from AGAE Technology, USA. The biosurfactant was delivered as a 90% pure product and was used without further purification. Surfactants such as cetyltrimethylammonium bromide (CTAB) and anionic sodium dodecyl sulphate (SDS) were purchased from Sigma-Aldrich and were of high purity.

2.4. Zeta potential measurements

The zeta potential of the mineral particles was determined with Zetasizer 2000 (Malvern, United Kingdom). The calibration was made applying a standard (DTS5050, Malvern instruments). Before each use, the cell was rinsed with HPLC grade water to ensure measurement stability. 1 µg of Wiśniówka mineral powder was added to 50 cm^3 of a solution in the pH range of 1-12. After 24 hours, the pH of the suspension was checked, and a measurement was carried out. The electrophoretic mobility of the particles was measured and converted into the zeta potential by the Smoluchowski equation. The influence of the surfactant and biosurfactant concentration on the zeta potential of the mineral particles was investigated at three pH values. The zeta potential analyses were performed for suspensions with a constant ionic strength equal to 10^{-3} M NaCl. All experiments were carried out at a stable measurement temperature of 25 °C. The zeta potential values were calculated from the mean of five separate runs, five measurements each.

2.5. Adhesion measurements

The experiments on jarosite adhesion to the mineral surface were conducted on a column analogous to the one for bioleaching. 50 g of mineral material (+0.8-1.2 mm) was used from the Wiśniówka Quarry. The mineral material was washed with distilled water at pH 2.5 for 24 h. Then, water was replaced with one litre of surfactant or biosurfactant solution at a concentration of 10^{-3} M. The ionic strength of the solution was 10^{-3} M NaCl. The solution flow was constant and equalled 17 cm^3 per minute. After 8 hours, 5 ml of concentrated jarosite suspension (50 mg/dm^3) was added to the column. Samples of suspension passing through the column were collected within 30 minutes of adding the jarosite. The concentration of jarosite in the collected suspension was measured spectrophotometrically.

2.6. Jarosite suspension stability

The suspension stability analysis was performed with various cationic and anionic surfactants and rhamnolipid concentrations. Jarosite suspensions were prepared in 20 ml glass cells. Measurements were carried out with Turbiscan® Lab (France). The stability of jarosite suspensions was correlated to the Turbiscan Stability Index (TSI), a parameter that allows comparing and characterizing the physical stability of various formulations. It is a numerical value that illustrates how fast the particles in suspension settle out and is determined based on backscattering profiles.

$$TSI = \sqrt{\frac{\sum_i^n (x_i - x_A)^2}{n-1}} \tag{1}$$

Where: x_i is the average value of the scattering light intensity at each measurement time, x_A is the average of x_i, and n is the number of scanning. The lower the TSI value is, the more stable the suspension.

2.7. Bioleaching experiment

Bioleaching was carried out in a 43 cm high glass column with an outflow providing a constant level of leaching solution, which was fed to the top by a peristaltic pump and regulated by a valve located at the bottom (Fig. 4). The outgoing solution was recirculated in the bed for effective leaching. 50 g of mineral material (0.8 – 1.2 mm) from the Wiśniówka Quarry was placed in the column. The mineral material was treated with 500 ml of 9K medium for 3 hours to stabilize the pH. Then 150 ml of *A. ferrooxidans* inoculum was added to the column. To modify the mineral material with surfactants, the bed was pretreated with a solution of the surface-active compound at a concentration of 3 mM and the same ionic strength for 24 hours. Next, the liquid was removed from the column and replaced with a 9K medium. The subsequent procedure was the same as without surfactant. During bioleaching, the Eh, pH was measured. The arsenic concentration was determined using the inductively coupled plasma-optical emission spectrometry technique (Agilent 5110 ICP-OES).

3. Results and discussion

The zeta potential measurements confirmed changes in the surface properties of minerals modified by surfactants. It is generally accepted that zeta potentials up to 30 and -30 mV are the limit potentials that

ensure the stability of the colloid (Tucker et al., 2015). As shown in Fig. 5, the jarosite zeta potential is small at the tested pH with a maximum of 16.5 mV at pH 3.22. The isoelectric point was not observed. The electropositive surface of jarosite at a pH below 4.0 was also reported by Sadowski (Sadowski et al., 2001) and Smeaton (Smeaton, 2012). In a highly acidic environment, the $FeOH^+$ groups of jarosite predominate over the FeO^- groups. Therefore, the surface has a net positive charge (Picazo-Rodríguez et al., 2022).
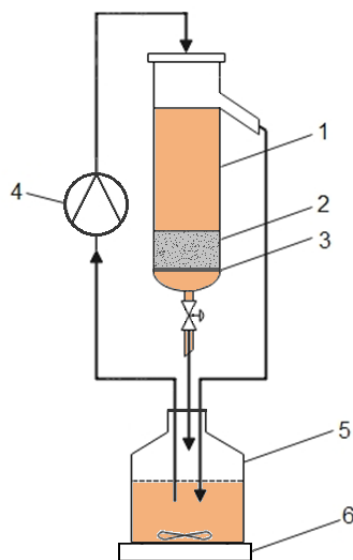

Fig. 4. Experimental setup: 1. Leaching solution; 2. Mineral waste; 3. Glass frit; 4. Peristaltic pump; 5. Feed/overflow container; 6. Magnetic stirrer with a heating plate
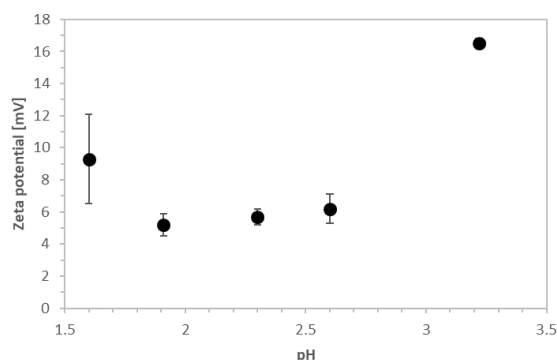

Fig. 5. Zeta potential of jarosite, ionic strength 10^{-3} M NaCl

The zeta potential of jarosite in the presence of surfactants and RL is depicted in Fig. 6a. At low concentrations of CTAB (0.1 – 0.3 mM), its adsorption led to a slight increase in the zeta potential of the secondary product (from 6.2 mV to 23.3 mV) arising from the presence of a positively charged head groups of the CTAB moiety. It was maintained at a level of approximately 52 mV for higher concentrations. The constant zeta potential value suggests no free active sites on the solid surface. Therefore, due to hydrophobic interactions between the surfactant tails, the formation of a surfactant bilayer could occur. The reported CMC of CTAB is 0.9-1.0 mM (Irfan et al., 2014; Li et al., 2006); thus, for the highest concentration, the excess surfactant might also be used to form micelles (Khademi et al., 2017).

Since the electrostatic repulsion occurs between the cationic surfactant and the jarosite surface, one possible mechanism assumes CTAB cation head (N^+-$(CH_3)_3$) group adsorption through Cl^- originating from the electrolyte solution. Fig. 7 schematically illustrates the possible adsorption of the investigated surfactants at the solid/liquid interface over concentration.
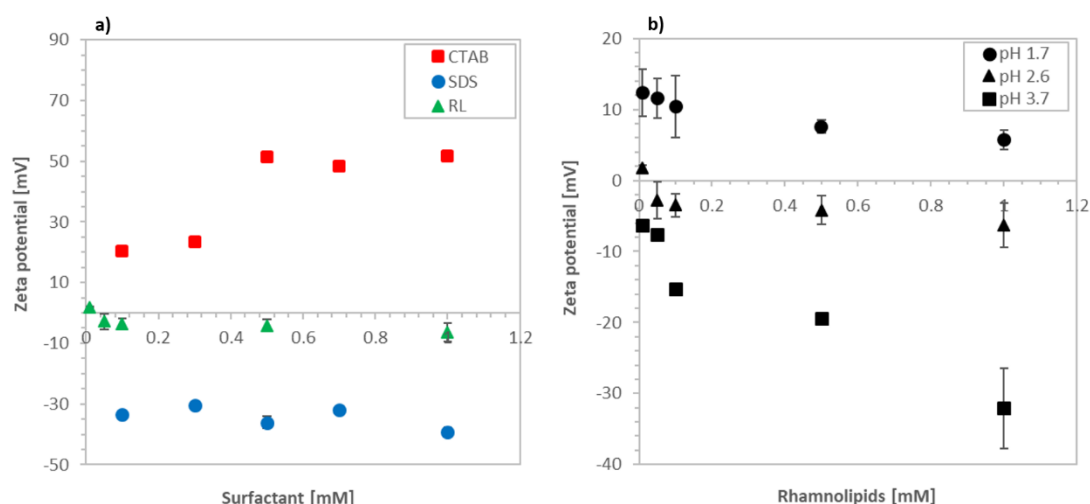
Fig. 6. Zeta potential of jarosite in the presence of a) CTAB, SDS and RL (pH 2.6) and b) effect of the rhamnolipids concentration on zeta potential of jarosite at different pH
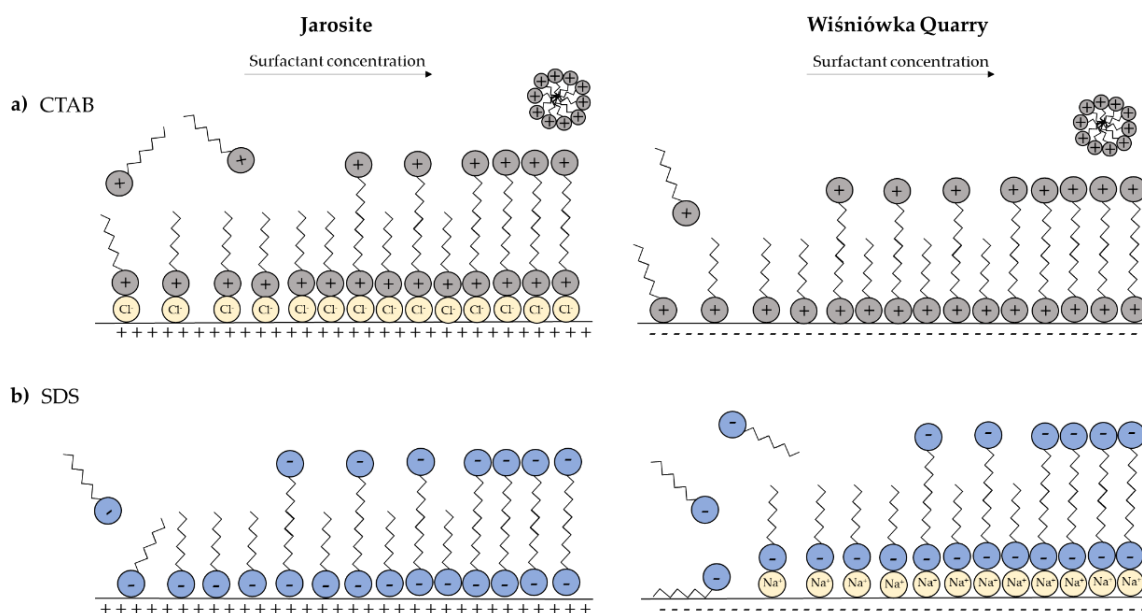

Fig. 7. Illustration of possible interaction of surfactants with jarosite and Wiśniówka Quarry mineral material surface in an electrolyte solution: a) CTAB and b) SDS

The addition of the SDS had the opposite effect. Negatively charged sulfate polar heads interact with the $FeOH^+$ group of the jarosite, shifting the zeta potential toward negative values (-30 mV). Probably, due to bilayer formation (Fig. 7), the total surface charge remains constant within the tested concentration range. In such a case, less surfactant is available for adsorption, and the zeta potential remains unchanged despite the increase in SDS concentration (Khademi et al., 2017). As the CMC value of the SDS is around 7 mM depending on the conditions (Jonsson et al., 1998), the formation of micelles should not occur.

The zeta potential of jarosite at pH 1.7 modified by RL was positive and slightly decreased with increasing biosurfactant concentrations (Fig. 6b). In a strongly acidic solution, the surface activity of rhamnolipids decreases markedly (Gogoi et al., 2016; Shreve and Makula, 2019). In the case of pH 2.6 and 3.7, the zeta potential shifted towards negative values. The acid dissociation constant of rhamnolipids in aqueous solutions ranges from 4.28 (±0.16) to 5.50 (±0.06) depending on the concentration (Lebrón-Paler et al., 2006). It suggests that in a highly acidic environment, the carboxyl group of the rhamnolipid is almost totally protonated and exhibits nonionic behaviour in aqueous

solutions (Ishigami et al., 1993). However, the results of the zeta potentiometric measurements shifted the initial positive surface charge of the jarosite toward negative values, suggesting that not all of the rhamnolipid carboxylate groups were deprotonated. The literature values for the CMC of different heterogeneous RL mixtures range from 50 to 200 mg/L, corresponding to approximately 0.08 to 0.23 mM (Christofi and Ivshina, 2002), therefore in tested biosurfactant concentration range multiple conformations on the surface are possible including micelles, vesicles, or lamella (Lebrón-Paler et al., 2006) .

The zeta potential of the mineral material from the Wiśniówka Quarry had a negative value in the pH range corresponding to the measurements of bioleaching and adhesion. The increase in the pH of the mineral suspension caused a systematic increase in the negative value of the zeta potential (Fig. 8). The negative potential value is most likely due to the presence of SiO^- groups derived from silica, the main component of the mineral material.
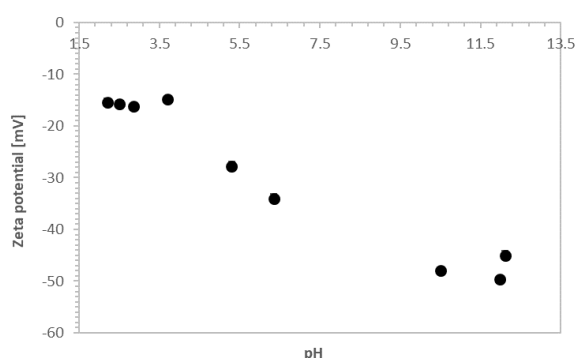

Fig. 8. Zeta potential of Wiśniówka Quarry material as a function of pH (ionic strength 10^{-3} M NaCl)

CTAB adsorption onto mineral from Wiśniówka Quarry is based on the electrostatic interaction between the cationic surfactant and the negatively-charged Wiśniówka particles' surface (Fig. 9a). The SiO^- anion present on the solid surface interacts with the CTAB (N^+-$(CH_3)_3$) charged cation head group. Since the zeta potential remains almost constant within the tested concentration range, it is possible that adsorption-related processes were saturated. It resulted in layer/bilayer formation (Fig. 7). Further surfactant addition was probably consumed by micellization.
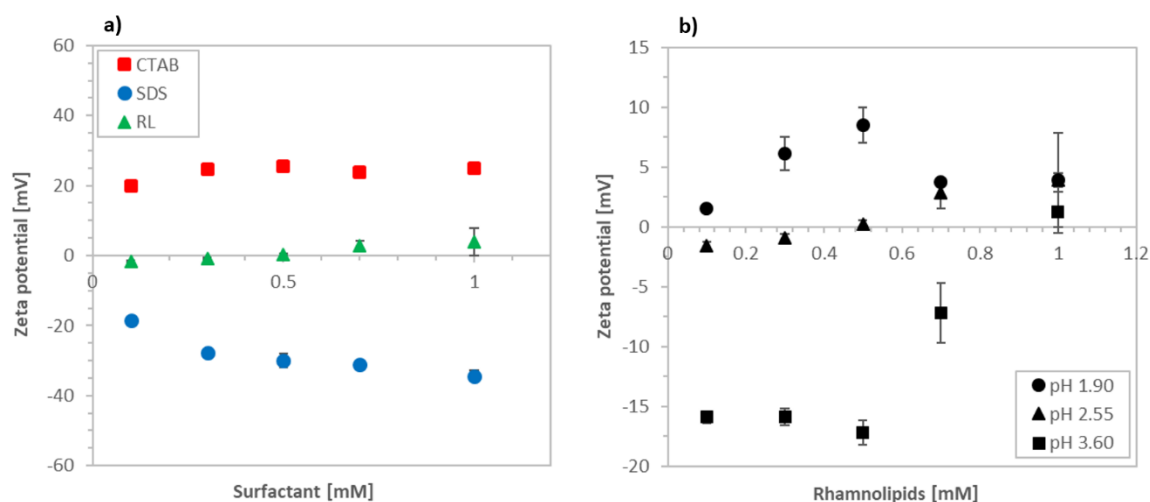

Fig. 9. Zeta potential of Wiśniówka material a) for various concentrations of CTAB (pH 2.5), SDS (pH 2.6) and RL (pH 2.5), b) for rhamnolipids at various pH

The addition of SDS at a concentration of 0.1 mM barely affected zeta potential (Fig. 9a). As the concentration increased, the zeta potential shifted toward more negative values, with the most significant change taking place for the concentration of 1 mM (from -15.8 mV to -39.2 mV). Negatively charged SiO^- groups of mineral waste bind the Na^+ cations present in the solution through attractive

electrostatic interactions. Then, negative SDS sulfate groups adsorb on the Na⁺ ion layer, resulting in the carbon chain being oriented upward. Carbon chains are bonded by the van der Waals force and form a bilayer (Shen and Lee, 2017). In this case, the negatively charged polar head increases the negative charge density and the absolute zeta potential. SDS was also proven to adsorb in strongly acidic pH on negatively charged surfaces, such as silica, with hydrophobic interaction since it has a hydrophobic surface on siloxane groups (Li and Ishiguro, 2016).

Modification of Wiśniówka particles by RL in strongly acidic conditions changed the zeta potential towards positive values (Fig. 9b). The biosurfactant molecules tended to aggregate due to greater intermolecular interactions between the biosurfactant species as their charge was reduced. At low pH, lamellar phases may occur (Lebrón-Paler et al., 2006). As mentioned earlier, RL exhibits the properties of a nonionic surfactant under strongly acidic conditions. The reduction of the negative potential of particles as a result of adsorption of the nonionic surfactant was previously reported by Somasundaran (Somasundaran et al., 1992). It implies that more than one mechanism is involved in RL adsorption on the surface of the solids studied. The strong surface-active properties of rhamnolipids, the presence of multiple biosurfactant congeners, and the dependence of the morphology of aggregates on the pH of the solution make it extremely difficult to determine the exact effect of rhamnolipids on such complex systems, based only on electrokinetic studies. Therefore, more detailed studies are planned.

The influence of surfactants and RL on the stability of the jarosite suspensions, expressed by the Turbiscan Stability Index (TSI) over time, is presented in Fig. 10. It is assumed that the higher the TSI value, the lower the stability of the colloid suspension. The analyses were conducted under conditions similar to bioleaching and adhesion tests (pH close to 2.5, ionic strength 10^{-3} M NaCl). As depicted in Fig. 10a, the jarosite particles tend to aggregate at low CTAB concentrations (0.05 and 0.1 M). The suspension became stable for 0.5 mM and higher. It can be driven by electrostatic repulsion between positive surface groups. The large positive zeta potential of jarosite (51.8 mV) in the presence of cationic surfactant (CTAB) explains the stability of this suspension. When sodium dodecyl sulphate (SDS) is present (Fig. 10b), an increased sedimentation level is observed at lower concentrations. The TSI index decreased significantly at a concentration of 1.0 mM, indicating the suspension's stability. The presence of rhamnolipids in jarosite suspension (Fig. 10c) causes destabilization, which is strongest at the highest biosurfactant concentration. It probably results from hydrophobic interaction between the hydrocarbon chains of adsorbed rhamnolipids molecules.
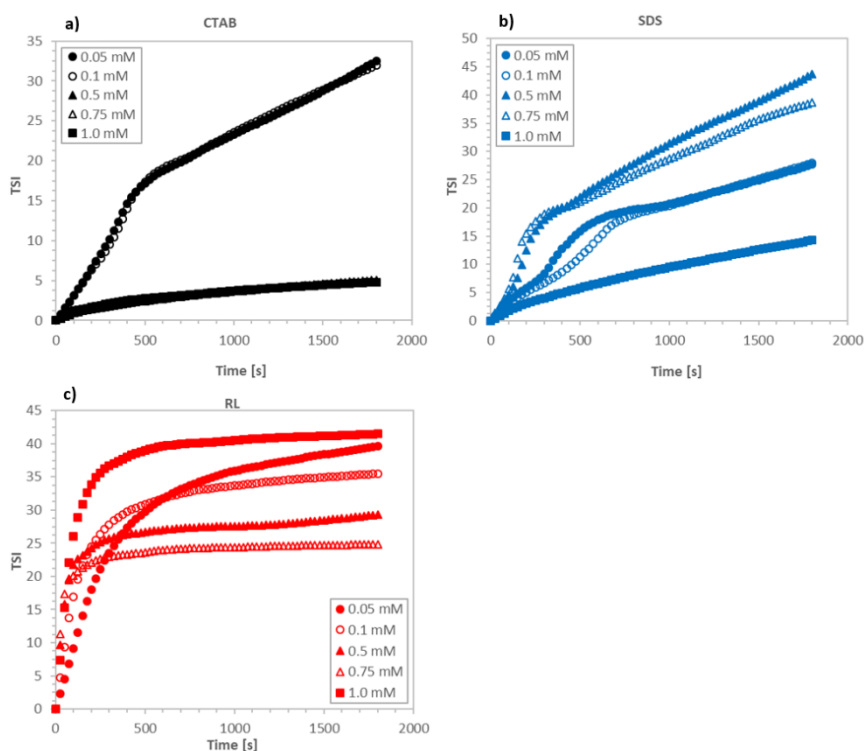

Fig. 10. Turbiscan Stability Index (TSI) of secondary product in the presence of a) CTAB, b) SDS, c) RL

In the bioleaching of sulfide and arsenic minerals, secondary products are formed parallel with primary mineral leaching. Jarosite $KFe_3(SO_4)_2(OH)_6$, schwertmannite $Fe_8O_8(OH)_6SO_4$, ferrihydrite $Fe_2O_3 \cdot 1.8H_2O$, goethite α-FeOOH, akaganeite β-FeOOH, lepidocrocite γ-FeOOH have been shown to form during chalcopyrite oxidation (Sasaki et al., 2009). When bioleaching is carried out in a heap, secondary minerals can adhere to the surface of the primary minerals, often inhibiting the process. The action of surfactants and biosurfactants affects adhesion and indirectly bio-extraction. The redox potential, indicating the oxidative activity of the bacteria (Table 3), showed similar values for all the systems studied. The final values ranged from 567 to 570 mV, suggesting that the presence of surfactants does not inhibit microbial activity. The successive decrease in pH also indicates the progress of bioleaching.

Fig. 11a shows the results of the bacterial leaching of the Wiśniówka solid in the presence of surfactants and rhamnolipids. A significant improvement in arsenic recovery was revealed in the presence of the cationic surfactant (CTAB). A slightly higher amount of As leached than that in the control sample was also observed for SDS. In the case of RL, the leaching efficiency followed that of Wiśniówka without modifications.

Table 3. pH and Eh values during bioleaching

| Time [days]	pH				Eh [mV]			
	W	W+CTAB	W+SDS	W+RL	W	W+CTAB	W+SDS	W+RL
1	2.56	2.52	2.59	2.54	404	372	403	403
4	2.68	2.47	2.54	2.38	422	387	418	588
5	2.26	2.47	2.51	2.35	574	402	478	590
6	2.28	2.46	2.41	2.32	571	417	554	587
7	2.26	2.45	2.34	2.27	569	4.36	558	584
8	2.25	2.37	2.3	2.21	568	543	556	581
11	2.21	2.21	2.22	2.16	563	565	553	575
12	2.19	2.16	2.18	2.17	552	564	554	573
13	2.17	2.2	2.24	2.15	550	565	553	571
14	2.18	2.15	2.2	2.15	551	563	556	568
18	2.17	2.09	2.17	2.08	549	562	554	567
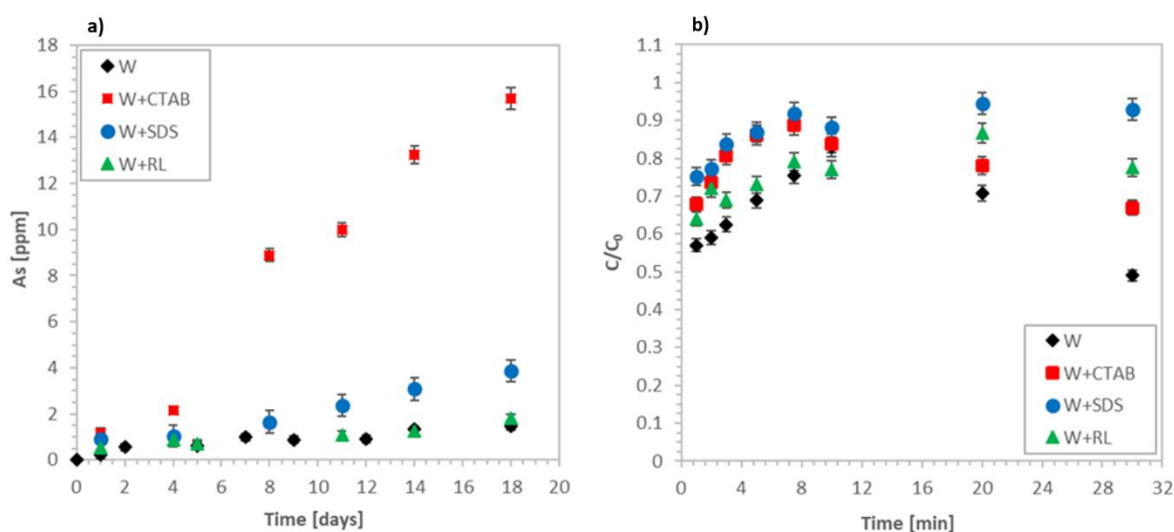
Fig. 11. a) Arsenic recovery from Wiśniówka (W) Quarry material in the presence of cetyltrimethylammonium bromide (CTAB), sodium dodecyl sulphate (SDS), and rhamnolipids (RL); b) jarosite adhesion onto the mineral surface

The leaching and bioleaching are carried out on the solid (mineral) surface. For this reason, the physicochemical parameters of this surface are essential for the course of bio-extraction. Furthermore, the interaction of bacteria cells with the surface of the mineral plays an important role in bioleaching (Diao et al., 2014). The adhesion of bacterial cells to the mineral surface is a complex process associated with biofilm formation (Su et al., 2020), in which extracellular polymeric substances (EPS) play an essential role (Li et al., 2016). The presence of secondary products in the leaching environment can interfere with biofilm formation. Therefore, competition in the adhesion on the mineral surface between jarosite and bacterial might occur. Table 4 presents the values of the measured zeta potentials of solid materials, stability (TSI), and adhesion data.

Table 4. Summary of surface parameters (pH 2.6, (bio)surfactant concentration 1mM)

Surfactant	Primary material (Wiśniówka)	Secondary product (jarosite)		Adhesion
	ζ [mV]	ζ [mV]	TSI	C/C_0
-	-15.8	6.2	58.4	0.49
CTAB	25.1	51.8	4.81	0.659
SDS	-34.4	-39.2	14.25	0.929
RL	9.9	15.1	41.46	0.776

High arsenic recovery when CTAB is adsorbed on the solid surface is probably related to the minimization of surface coverage by secondary minerals. As the surface of Wiśniówka particles is positively charged (25.1 mV), the jarosite (6.2 mV) is less likely to adhere. The second factor in improving the effectiveness of bioleaching is the immobilization of bacteria cells on the surface of minerals, having favourable conditions to adhere. The low As recovery for the unmodified material might result from adhesion of the jarosite, which inhibits the process. Electrokinetic measurements do not support the influence of SDS and RL on As recovery. In bioleaching, we deal with many factors that affect the adhesion of both secondary products and bacterial cells. The zeta potential results do not reflect the existing impacts fully, as other interactions might compensate for the weak electrostatic interaction. Therefore, detailed studies are still necessary to be conducted.

Research on the adhesion of jarosite particles to the mineral surface (Fig. 11b) has shown the highest adhesion for the unmodified surface of the bed, which is substantiated by bioleaching. Lower adhesion occurs when a surface-active compound is used. Those results are not consistent with bio-extraction. However, it should be noted that the time during which the adhesion of the secondary products in the bed was carried out was short and refers only to the initial phase of bioleaching. Assuming the presence of bio- and surfactant molecules in the leaching solution, very low adhesion of jarosite to the surface of primary minerals will be observed in the presence of all tested surface-active compounds due to the strong repulsion between two oppositely charged objects (i.e. for SDS -39.2 mV jarosite and -34.4 mV minerals). The best conditions for adhesion will be in the absence of added reagents which reflects the results depicted in Fig. 11b. Under these conditions, there is an electrostatic attraction between the primary mineral (-15.8 mV) and the jarosite particles (6.2 mV).

4. Conclusions

Modifying mineral surfaces with surfactants might be a tool to prevent unwanted effects of bioleaching. This study demonstrated that surface-active compounds change the surface properties of tested solids and do not inhibit bacterial growth. CTAB caused a shift in the zeta potential towards positive values, while the presence of SDS decreased the zeta potential. The best arsenic recovery of the mineral material from the Wiśniówka Quarry was achieved in the presence of cationic surfactant. It is associated with the immobilization of bacterial cells on positively charged particles and preventing adhesion of the secondary product (jarosite). The cationic surfactant (CTAB) above the 0.5 mM concentration caused the stability of the jarosite suspension due to the strong electrostatic interaction between the particle of jarosite (the zeta potential of the jarosite equals 51.8 mV). It was also shown that surface-active

compounds do not significantly facilitate the adhesion of the jarosite to the surface of the leached mineral material.

Acknowledgements

References

AKCIL, A., KOLDAS, S., 2006. *Acid Mine Drainage (AMD): causes, treatment and case studies.* Journal of Cleaner Production. 12-13, 1139-1145.

CAETANO, M.L., CIMINELLI, V.S.T., ROCHA, S.D.F., SPITALE, M.C., CALDEIRA, C.L., 2009. *Batch and continuous precipitation of scorodite from dilute industrial solutions.* Hydrometallurgy 95, 1-2, 44-52.

CHRISTOFI, N., IVSHINA, I.B., 2002. *Microbial surfactants and their use in field studies of soil remediation.* Journal of Applied Microbiology 93, 6, 915-929.

DAOUD, J., KARAMANEV, D., 2006. *Formation of jarosite during Fe^{2+} oxidation by Acidithiobacillus ferrooxidans.* Minerals Engineering 19, 9, 960-967.

DELIYANNI, E.A., BAKOYANNAKIS, D.N., ZOUBOULIS, A.I., MATIS, K.A., NALBANDIAN, L., 2001. *Akaganéite-type β-FeO(OH) nanocrystals: Preparation and characterization.* Microporous and Mesoporous Materials 42, 1, 49-57.

DIAO, M., TARAN, E., MAHLER, S., NGUYEN, A. V., 2014. *A concise review of nanoscopic aspects of bioleaching bacteria-mineral interactions.* Advances in Colloid and Interface Science 212, 45-63.

DOLD, B., 2017. *Acid rock drainage prediction: A critical review.* Journal of Geochemical Exploration 172, 120-132.

DRAHOTA, P., FILIPPI, M., 2009. *Secondary arsenic minerals in the environment: A review.* Environment International 35, 8, 1243-1255.

EGAL, M., CASIOT, C., MORIN, G., PARMENTIER, M., BRUNEEL, O., LEBRUN, S., ELBAZ-POULICHET, F., 2009. *Kinetic control on the formation of tooeleite, schwertmannite and jarosite by Acidithiobacillus ferrooxidans strains in an As(III)-rich acid mine water.* Chemical Geology 265, 3-4, 432-441.

GOGOI, D., BHAGOWATI, P., GOGOI, P., BORDOLOI, N.K., RAFAY, A., DOLUI, S.K., MUKHERJEE, A.K., 2016. *Structural and physico-chemical characterization of a dirhamnolipid biosurfactant purified from: Pseudomonas aeruginosa: Application of crude biosurfactant in enhanced oil recovery.* RSC Advances 6, 70669-70681.

HAMMARSTROM, J.M., SEAL, R.R., MEIER, A.L., KORNFELD, J.M., 2005. *Secondary sulfate minerals associated with acid drainage in the eastern US: Recycling of metals and acidity in surficial environments.* Chemical Geology 215, 407–431.

HOUNGALOUNE, S., KAWAAI, T., HIROYOSHI, N., ITO, M., 2014. *Study on schwertmannite production from copper heap leach solutions and its efficiency in arsenic removal from acidic sulfate solutions.* Hydrometallurgy 147–148, 30-40.

IRFAN, M., USMAN, M., MANSHA, A., RASOOL, N., IBRAHIM, M., RANA, U.A., SIDDIQ, M., ZIA-UL-HAQ, M., JAAFAR, H.Z.E., KHAN, S.U.D., 2014. *Thermodynamic and Spectroscopic Investigation of Interactions between Reactive Red 223 and Reactive Orange 122 Anionic Dyes and Cetyltrimethyl Ammonium Bromide (CTAB) Cationic Surfactant in Aqueous Solution.* Scientific World Journal 2014, 1-8.

ISHIGAMI, Y., GAMA, Y., ISHII, F., CHOI, Y.K., 1993. *Colloid Chemical Effect of Polar Head Moieties of a Rhamnolipid-Type Biosurfactant.* Langmuir 9, 1634-1636.

JOHNSON, D.B., HALLBERG, K.B., 2005. *Acid mine drainage remediation options: A review.* Science of the Total Environment 338, 1-2, 3-14.

JONSSON, B., LINDMAN, B., HOLMBERG, K., 1998. *Surfactants and polymers in aqueous solutions.* IEEE Electrical Insulation Magazine 14. https://doi.org/10.1109/MEI.1998.714652

JÖNSSON, J., PERSSON, P., SJÖBERG, S., LÖVGREN, L., 2005. *Schwertmannite precipitated from acid mine drainage: Phase transformation, sulphate release and surface properties.* Applied Geochemistry 20, 1, 179-191.

JÖNSSON, JÖRGEN, JÖNSSON, JULIA, LÖVGREN, L., 2006. *Precipitation of secondary Fe(III) minerals from acid mine drainage.* Applied Geochemistry 21, 3, 437-445.

KAKSONEN, A.H., MORRIS, C., REA, S., LI, J., USHER, K.M., MCDONALD, R.G., HILARIO, F., HOSKEN, T., JACKSON, M., DU PLESSIS, C.A., 2014. *Biohydrometallurgical iron oxidation and precipitation: Part II - Jarosite precipitate characterisation and acid recovery by conversion to hematite.* Hydrometallurgy 147–148, 264-272.

KHADEMI, M., WANG, W., REITINGER, W., BARZ, D.P.J., 2017. *Zeta Potential of Poly(methyl methacrylate) (PMMA) in Contact with Aqueous Electrolyte-Surfactant Solutions.* Langmuir 33, 40, 10473-10482.

LEBRÓN-PALER, A., PEMBERTON, J.E., BECKER, B.A., OTTO, W.H., LARIVE, C.K., MAIER, R.M., 2006. *Determination of the acid dissociation constant of the biosurfactant monorhamnolipid in aqueous solution by potentiometric and spectroscopic methods.* Analytical Chemistry 78, 22, 7649-7658.

LEE, J.S., CHON, H.T., 2006. *Hydrogeochemical characteristics of acid mine drainage in the vicinity of an abandoned mine, Daduk Creek, Korea.* Journal of Geochemical Exploration 88, 1, 37-40.

LI, P., ISHIGURO, M., 2016. *Adsorption of anionic surfactant (sodium dodecyl sulfate) on silica.* Soil Science and Plant Nutrition 62, 3, 223-229.

LI, W., ZHANG, M., ZHANG, J., HAN, Y., 2006. *Self-assembly of cetyl trimethylammonium bromide in ethanol-water mixtures.* Frontiers of Chemistry in China 1, 438-442.

PAIKARAY, S., 2015. *Arsen-Geochemie von Acid Mine Drainage.* Mine Water and the Environment 34, 181-196.

PAWLOWSKA, A., SADOWSKI, Z., 2020. *Effect of schwertmannite surface modification by surfactants on adhesion of acidophilic bacteria.* Microorganisms 8, 11, 1725-1737.

PICAZO-RODRÍGUEZ, N.G., CARRILLO-PEDROZA, F.R., SORIA-AGUILAR, M. DE J., BALTIERRA, G., GONZÁLEZ, G., MARTINEZ-LUEVANOS, A., GUZMÁN, I.A., 2022. *Use of Thermally Modified Jarosite for the Removal of Hexavalent Chromium by Adsorption.* Crystals (Basel) 12, 1, 80-91.

SADOWSKI, Z., POLOWCZYK, I., FARBISZEWSKA, T., FARBISZEWSKA-KICZMA, J., 2001. *Adhesion of jarosite particles to the mineral surface*, in: Prace Naukowe Instytutu Gornictwa Politechniki Wroclawskiej.

SASAKI, K., NAKAMUTA, Y., HIRAJIMA, T., TUOVINEN, O.H., 2009. *Raman characterization of secondary minerals formed during chalcopyrite leaching with Acidithiobacillus ferrooxidans.* Hydrometallurgy 95, 1-2, 153-158.

SHEN, Z.Y., LEE, M.T., 2017. *On the morphology of the SDS film on the surface of borosilicate glass.* Materials 10, 5, 555.

SHREVE, G.S., MAKULA, R., 2019. *Characterization of a new rhamnolipid biosurfactant complex from pseudomonas isolate DYNA270.* Biomolecules 9, 12, 885-896.

SMEATON, C., 2012. *Investigating the Susceptibility of Jarosite Minerals to Reductive Dissolution by a Dissimilatory Metal Reducing Bacterium* (Shewanella putrefaciens CN32). Electronic Theses and Dissertations. 450.

SOMASUNDARAN, P., SNELL, E.D., FU, E., XU, Q., 1992. *Effect of adsorption of nonionic surfactant and non-ionic-anionic surfactant mixtures on silica-liquid interfacial properties.* Colloids and Surfaces 63, 1-2, 49-54.

SU, G., DENG, X., HU, L., PRABURAMAN, L., ZHONG, H., HE, Z., 2020. *Comparative analysis of early-stage adsorption and biofilm formation of thermoacidophilic archaeon Acidianus manzaensis YN-25 on chalcopyrite and pyrite surfaces.* Biochemical Engineering Journal 163, 107744.

TUCKER, I.M., CORBETT, J.C.W., FATKIN, J., JACK, R.O., KASZUBA, M., MACCREATH, B., MCNEIL-WATSON, F., 2015. *Laser Doppler Electrophoresis applied to colloids and surfaces.* Current Opinion in Colloid and Interface Science 20, 4, 215-226.